

5.4 Mean Kinetic Energy and Its Interaction with Turbulence

Term IV in the TKE budget (5.1) involves the production of TKE by interaction of turbulence with the mean wind. One might expect that the production of TKE is accompanied by a corresponding loss of kinetic energy from the mean flow.

To study that possibility, start with the prognostic equation for mean wind in turbulent flow (3.4.3c), multiply by \bar{U}_i , and use the chain rule to derive the following equation for mean kinetic energy per unit mass [$MKE/m = 0.5(\bar{U}^2 + \bar{V}^2 + \bar{W}^2) = 0.5 \bar{U}_i^2$]:

$$\frac{\partial(0.5\bar{U}_i^2)}{\partial t} + \bar{U}_j \frac{\partial(0.5\bar{U}_i^2)}{\partial x_j} = -g\delta_{i3}\bar{U}_i + f\epsilon_{ij3}\bar{U}_i\bar{U}_j - \frac{\bar{U}_i}{\rho} \frac{\partial\bar{P}}{\partial x_i} + v\bar{U}_i \frac{\partial^2\bar{U}_i}{\partial x_j^2} - \bar{U}_i \frac{\partial(\overline{u_i' u_j'})}{\partial x_j} \tag{5.4a}$$

- | | | | | | | |
|----------------------------|--|--|--|--|---|---|
| I | II | III | IV | V | VI | X |
| Term I | Term II | Term III | Term IV | Term V | Term VI | Term X |
| represents storage of MKE. | describes the advection of MKE by the mean wind. | indicates that gravitational acceleration of vertical motions alter the MKE. | shows the effects of the Coriolis force. | represents the production of MKE when pressure gradients accelerate the mean flow. | represents the molecular dissipation of mean motions. | indicates the interaction between the mean flow and turbulence. |

When the Coriolis term (IV) is summed over all values of the repeated indices, the result equals zero. This confirms our observation that Coriolis force can neither create nor destroy energy; it merely redirects the winds. Using the product rule, the last term (X) can be rewritten as

$$-\bar{U}_i \frac{\partial(\overline{u_i' u_j'})}{\partial x_j} = \overline{u_i' u_j'} \frac{\partial\bar{U}_i}{\partial x_j} - \frac{\partial(\overline{u_i' u_j'} \bar{U}_i)}{\partial x_j}$$

This leaves

$$\frac{\partial(0.5\bar{U}_i^2)}{\partial t} + \bar{U}_j \frac{\partial(0.5\bar{U}_i^2)}{\partial x_j} = -g\bar{W} - \frac{\bar{U}_i}{\rho} \frac{\partial\bar{P}}{\partial x_i} + v\bar{U}_i \frac{\partial^2\bar{U}_i}{\partial x_j^2} + \overline{u_i' u_j'} \frac{\partial\bar{U}_i}{\partial x_j} - \frac{\partial(\overline{u_i' u_j'} \bar{U}_i)}{\partial x_j} \tag{5.4b}$$

If we compare the TKE equation (5.1) with the MKE equation (5.4b):

$$\frac{\partial(TKE/m)}{\partial t} = \dots - \overline{u_i' u_j'} \frac{\partial\bar{U}_i}{\partial x_j}$$

$$\frac{\partial(MKE/m)}{\partial t} = \dots + \overline{u_i' u_j'} \frac{\partial\bar{U}_i}{\partial x_j}$$

we see that they both contain a term describing the interaction between the mean flow and turbulence. The sign of these terms differ. *Thus, the energy that is mechanically produced as turbulence is lost from the mean flow, and vice versa.*

5.5 Stability Concepts

Unstable flows become or remain turbulent. Stable flows become or remain laminar. There are many factors that can cause laminar flow to become turbulent, and other factors that tend to stabilize flows. If the net effect of all the destabilizing factors exceeds the net effect of the stabilizing factors, then turbulence will occur. In many cases, these factors can be interpreted as terms in the TKE budget equation.

To simplify the problem, investigators have historically paired one destabilizing factor with one stabilizing factor, and expressed these factors as a dimensionless ratio. Examples of these ratios are the Reynolds number, Richardson number, Rossby number, Froude number, and Rayleigh number. Some other stability parameters such as static stability, however, are not expressed in dimensionless form.

5.5.1 Static Stability and Convection

Static stability is a measure of the capability for buoyant convection. The word "static" means "having no motion"; hence this type of stability does not depend on wind. Air is statically unstable when less-dense air (warmer and/or moister) underlies more-dense air. The flow responds to this instability by supporting convective circulations such as thermals that allow buoyant air to rise to the top of the unstable layer, thereby stabilizing the fluid. Thermals also need some trigger mechanism to get them started. In the real boundary layer, there are so many triggers (hills, buildings, trees, dark fields, or other perturbations to the mean flow) that convection is usually insured, given the static instability.

Local Definitions. The traditional definition taught in basic meteorology classes is local in nature; namely, the static stability is determined by the local lapse rate. The local definition frequently fails in convective MLs, because the rise of thermals from near the surface or their descent from cloud top depends on their excess buoyancy and not on the ambient lapse rate.

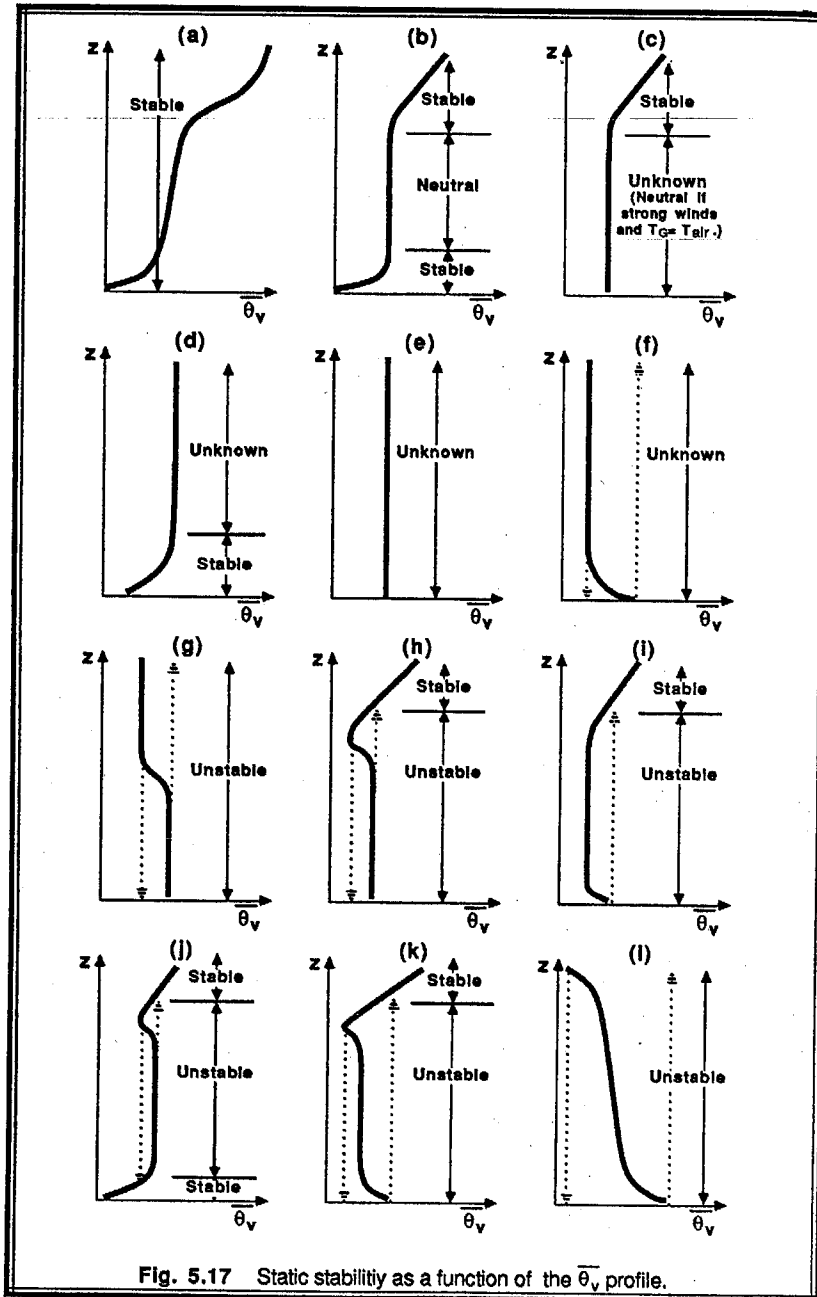


Fig. 5.17 Static stability as a function of the $\bar{\theta}_v$ profile.

As an example, in the middle 50% of the convective ML the lapse rate is nearly adiabatic, causing an incorrect classification of neutral stability if the traditional local definition is used. We must make a clear distinction between the phrases "adiabatic lapse rate" and "neutral stability". An *adiabatic lapse rate* (in the virtual potential temperature sense) may be statically stable, neutral, or unstable, depending on convection and the buoyancy flux. *Neutral stability* implies a very specific situation: adiabatic lapse rate AND no convection. The two phrases should NOT be used interchangeably, and the phrase "neutral lapse rate" should be avoided altogether.

We conclude that *measurement of the local lapse rate alone is INSUFFICIENT to determine the static stability*. Either knowledge of the whole $\bar{\theta}_v$ profile is needed (described next), or measurement of the turbulent buoyancy flux must be made.

Nonlocal Definitions. It is better to examine the stability of the whole layer, and make a layer determination of stability such as was done in section 1.6.4. For example, if $\overline{w'\theta'_v}$ at the earth's surface is positive, or if displaced air parcels will rise from the ground or sink from cloud top as thermals traveling across a BL, then the whole BL is said to be *unstable or convective*. If $\overline{w'\theta'_v}$ is negative at the surface, or if displaced air parcels return to their starting point, then the BL is said to be *stable*.

If, when integrated over the depth of the boundary layer, the mechanical production term in the TKE equation (5.1) is much larger than the buoyancy term, or if the buoyancy term is near zero, then the boundary layer is said to be *neutral*. In some of the older literature, the boundary layer of this latter case is also sometimes referred to as an *Ekman boundary layer*. During fair weather conditions over land, the BL touching the ground is rarely neutral. Neutral conditions are frequently found in the RL aloft. In overcast conditions with strong winds but little temperature difference between the air and the surface, the BL is often close to neutral stability.

In the absence of knowledge of convection or measurements of buoyancy flux, an alternate determination of static stability is possible if the $\bar{\theta}_v$ profile over the whole BL is known, as sketched in Fig 5.17. As is indicated in the figure, if only portions of the profile are known, then the stability might be indeterminate. Also, it is clear that there are many situations where the traditional local definition fails.

5.5.2 Example

Problem. Given the sounding at right, identify the static stability of the air at $z = 600$ m.

Solution. Using a local definition in the absence of heat fluxes, if we look downward from 600 m until a diabatic layer is encountered, we find a stable layer with cooler temperatures at 200 m. Before we reach any hasty conclusions, however, we must look up from 600 m. Doing so we find cooler unstable air at 1000 m. Thus, the static stability is unstable at 600 m.

Discussion. The whole adiabatic layer is unstable, considering the nonlocal approach of a cool parcel sinking from above. This sounding is characteristic of stratocumulus.

5.5.3 Dynamic Stability and Kelvin-Helmholtz Waves

The word "dynamic" refers to motion; hence, dynamic stability depends in part on the winds. Even if the air is statically stable, wind shears may be able to generate turbulence dynamically.

Some laboratory experiments have been performed (Thorpe, 1969, 1973; Woods 1969) using denser fluids underlying less-dense fluids with a velocity shear between the layers to simulate the stable stratification and shears of the atmosphere. Fig 5.18 is a sketch of the resulting flow behavior. The typical sequence of events is:

- (1) A shear exists across a density interface. Initially, the flow is laminar.
- (2) If a critical value of shear is reached (see section 5.6), then the flow becomes dynamically unstable, and gentle waves begin to form on the interface. The crests of these waves are normal to the shear direction.
- (3) These waves continue to grow in amplitude, eventually reaching a point where each wave begins to "roll up" or "break". This "breaking" wave is called a *Kelvin-Helmholtz (KH) wave*, and is based on different physics than surface waves that "break" on an ocean beach.
- (4) Within each wave, there exists some lighter fluid that has been rolled under denser fluid, resulting in patches of static instability. On radar, these features appear as braided ropelike patterns, "cat's eye" patterns or breaking wave patterns.
- (5) The static instability, combined with the continued dynamic instability, causes each wave to become turbulent.
- (6) The turbulence then spreads throughout the layer, causing a diffusion or mixing of the different fluids. During this diffusion process, some momentum is transferred between the fluids, reducing the shear between the layers. What was formerly a sharp, well-defined, interface becomes a broader, more diffuse shear layer with weaker shear and static stability.

- (7) This mixing can reduce the shear below a critical value and eliminate the dynamic instability.
- (8) In the absence of continued forcing to restore the shears, turbulence decays in the interface region, and the flow becomes laminar again.

This sequence of events is suspected to occur during the onset of *clear air turbulence (CAT)*. These often occur above and below strong wind jets, such as the nocturnal jet and the planetary-scale jet stream. In these situations, however, continued dynamic forcings can allow turbulence to continue for hours to days. These regions of CAT have large horizontal extent (hundreds of kilometers in some cases), but usually limited vertical extent (tens to hundred of meters). They can be visualized as large pancake-shaped regions of turbulence. Aircraft encountering CAT can often climb or descend into smoother air.

Although KH waves are probably a frequent occurrence within statically stable shear layers, they are only rarely observed with the naked eye. Occasionally, there is sufficient moisture in the atmosphere to allow cloud droplets to act as visible tracers. Clouds that form in the rising portions of the waves often form parallel bands called *billow clouds*. The orientation of these bands is perpendicular to the shear vector. One must remember that the wind SHEAR vector need not necessarily point in the same direction as the mean wind vector.

For both static and dynamic instabilities, and many other instabilities for that matter, it is interesting to note that the fluid reacts in a manner to undo the cause of the instability. This process is strikingly similar to *LeChatelier's principle* of chemistry, which states that "if some stress is brought to bear upon a system in equilibrium, a change occurs such that the equilibrium is displaced in a direction which tends to undo the effect of the stress". Thus, turbulence is a mechanism whereby fluid flows tend to undo the cause of the instability. In the case of static instabilities, convection occurs that tends to move more buoyant fluid upward, thereby stabilizing the system. For dynamic instability, turbulence tends to reduce the wind shears, also stabilizing the system.

With this in mind, it is apparent that turbulence acts to eliminate itself. After the unstable system has been stabilized, turbulence tends to decay. Given observations of turbulence occurring for long periods of time within the boundary layer, it is logical to surmise that there must be external forcings tending to destabilize the BL over long time periods. In the case of static instability, the solar heating of the ground by the sun is that external forcing. In the case of dynamic instabilities, pressure gradients imposed by synoptic-scale features drive the winds against the dissipative effects of turbulence.

By comparing the relative magnitudes of the shear production and buoyant consumption terms of the TKE equation, we can hope to estimate when the flow might become dynamically unstable. The Richardson number, Ri , described in the next subsection, can be used as just such an indicator.

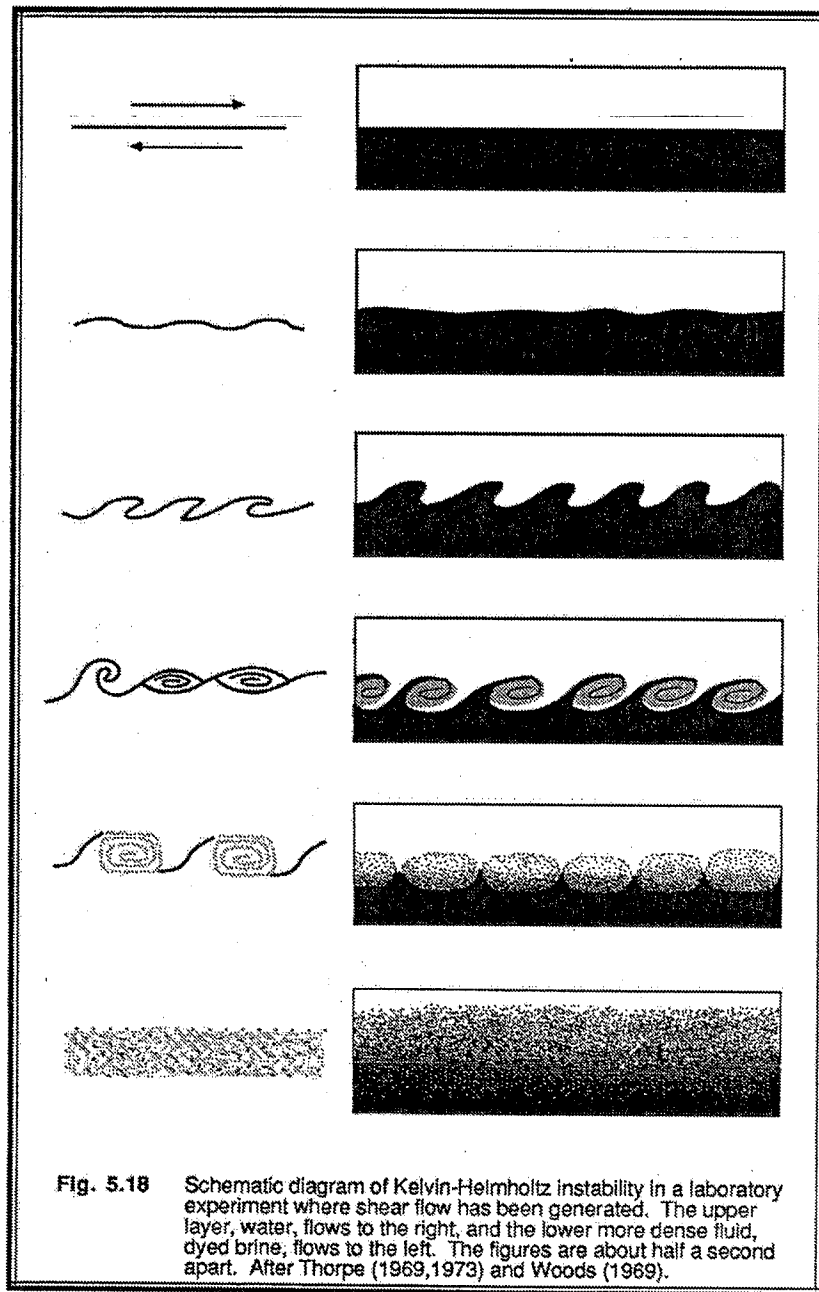


Fig. 5.18 Schematic diagram of Kelvin-Helmholtz instability in a laboratory experiment where shear flow has been generated. The upper layer, water, flows to the right, and the lower more dense fluid, dyed brine, flows to the left. The figures are about half a second apart. After Thorpe (1969,1973) and Woods (1969).

5.6 The Richardson Number

5.6.1 Flux Richardson Number

In a statically stable environment, turbulent vertical motions are acting against the restoring force of gravity. Thus, buoyancy tends to suppress turbulence, while wind shears tend to generate turbulence mechanically. The buoyant production term (Term III) of the TKE budget equation (5.1b) is negative in this situation, while the mechanical production term (Term IV) is positive. Although the other terms in the TKE budget are certainly important, a simplified but nevertheless useful approximation to the physics is possible by examining the ratio of Term III to Term IV. This ratio, called the *flux Richardson number*, R_f , is given by

$$R_f = \frac{\left(\frac{g}{\theta_v}\right) \overline{(w'\theta_v')}}{\overline{(u_i'u_j')} \frac{\partial U_i}{\partial x_j}} \quad (5.6.1a)$$

where the negative sign on Term IV is dropped by convention. The Richardson number is dimensionless. The denominator consists of 9 terms, as implied by the summation notation.

If we assume horizontal homogeneity and neglect subsidence, then the above equation reduces to the more common form of the flux Richardson number:

$$R_f = \frac{\left(\frac{g}{\theta_v}\right) \overline{(w'\theta_v')}}{\overline{(u'w')} \frac{\partial \bar{U}}{\partial z} + \overline{(v'w')} \frac{\partial \bar{V}}{\partial z}} \quad (5.6.1b)$$

For statically unstable flows, R_f is usually negative (remember that the denominator is usually negative). For neutral flows, it is zero. For statically stable flows, R_f is positive.

Richardson proposed that $R_f = +1$ is a critical value, because the mechanical production rate balances the buoyant consumption of TKE. At any value of R_f less than +1, static stability is insufficiently strong to prevent the mechanical generation of turbulence. For negative values of R_f , the numerator even contributes to the generation of turbulence. Therefore, he expected that

Flow IS turbulent (dynamically unstable) when $R_f < +1$

Flow BECOMES laminar (dynamically stable) when $R_f > +1$

We recognize that statically unstable flow is, by definition, always dynamically unstable.

5.6.2 Gradient Richardson Number

A peculiar problem arises in the use of R_f ; namely, we can calculate its value only for turbulent flow because it contains factors involving turbulent correlations like $\overline{w'\theta_v'}$. In other words, we can use it to determine whether turbulent flow will become laminar, but not whether laminar flow will become turbulent.

Using the reasoning of section 2.7 and Fig 2.13, it is logical to suggest that the value of the turbulent correlation $-\overline{w'\theta_v'}$ might be proportional to the lapse rate $\partial\overline{\theta_v}/\partial z$. Similarly, we might suggest that $-\overline{u'w'}$ is proportional to $\partial\overline{U}/\partial z$, and that $-\overline{v'w'}$ is proportional to $\partial\overline{V}/\partial z$. These arguments form the basis of a theory known as K-theory or eddy diffusivity theory, which will be discussed in much more detail in chapter 6. For now, we will just assume that the proportionalities are possible, and substitute those in (5.6.1b) to give a new ratio called the *gradient Richardson number*, Ri :

$$Ri = \frac{\frac{g}{\theta_v} \frac{\partial\overline{\theta_v}}{\partial z}}{\left[\left(\frac{\partial\overline{U}}{\partial z} \right)^2 + \left(\frac{\partial\overline{V}}{\partial z} \right)^2 \right]} \quad (5.6.2)$$

When investigators refer to a "Richardson number" without specifying which one, they usually mean the gradient Richardson number.

Theoretical and laboratory research suggest that laminar flow becomes unstable to KH-wave formation and the ONSET of turbulence when Ri is smaller than the *critical Richardson number*, R_c . Another value, R_T , indicates the termination of turbulence. The dynamic stability criteria can be stated as follows:

Laminar flow becomes turbulent when $Ri < R_c$.

Turbulent flow becomes laminar when $Ri > R_T$.

Although there is still some debate on the correct values of R_c and R_T , it appears that $R_c = 0.21$ to 0.25 and $R_T = 1.0$ work fairly well. Thus, there appears to be a *hysteresis* effect because R_T is greater than R_c .

One hypothesis for the apparent hysteresis is as follows. Two conditions are needed for turbulence: instability, and some trigger mechanism. Suppose that dynamic instability occurs whenever $Ri < R_T$. If one trigger mechanism is existing turbulence in or adjacent to the unstable fluid, then turbulence can continue as long as $Ri < R_T$ because of the presence of both the instability and the trigger. If KH waves are another trigger mechanism, then in the absence of existing turbulence one finds that Ri must get well

below R_T before KH waves can form. Laboratory and theoretical work have shown that the criterion for KH wave formation is $Ri < R_c$. This leads to the apparent hysteresis, because the Richardson number of nonturbulent flow must be lowered to R_c before turbulence will start, but once turbulent, the turbulence can continue until the Richardson number is raised above R_T .

5.6.3 Bulk Richardson Number

The theoretical work yielding $R_c \cong 0.25$ is based on local measurements of the wind shear and temperature gradient. Meteorologists rarely know the actual local gradients, but can approximate the gradients using observations made at a series of discrete height intervals. If we approximate $\partial\overline{\theta_v}/\partial z$ by $\Delta\overline{\theta_v}/\Delta z$, and approximate $\partial\overline{U}/\partial z$ and $\partial\overline{V}/\partial z$ by

$\Delta\overline{U}/\Delta z$ and $\Delta\overline{V}/\Delta z$ respectively, then we can define a new ratio known as the *bulk Richardson number*, R_B :

$$R_B = \frac{g \Delta\overline{\theta_v} \Delta z}{\theta_v [(\Delta\overline{U})^2 + (\Delta\overline{V})^2]} \quad (5.6.3)$$

It is this form of the Richardson number that is used most frequently in meteorology, because rawinsonde data and numerical weather forecasts supply wind and temperature measurements at discrete points in space. The sign of the finite differences are defined,

for example, by $\Delta\overline{U} = \overline{U}(z_{top}) - \overline{U}(z_{bottom})$.

Unfortunately, the critical value of 0.25 applies only for local gradients, not for finite differences across thick layers. In fact, the thicker the layer is, the more likely we are to average out large gradients that occur within small subregions of the layer of interest. The net result is (1) we introduce uncertainty into our prediction of the occurrence of turbulence, and (2) we must use an artificially large (theoretically unjustified) value of the critical Richardson number that gives reasonable results using our smoothed gradients. The thinner the layer, the closer the critical Richardson number will likely be to 0.25. Since data points in soundings are sometimes spaced far apart in the vertical, approximations such as shown in the graph and table in Fig 5.19 can be used to estimate the probability and intensity of turbulence (Lee, et al., 1979).

Table 5-1 shows a portion of a rawinsonde sounding, together with the corresponding values of bulk Richardson number. The resulting turbulence diagnosis is given in the rightmost column of Table 5-1. Note that the Richardson number itself says nothing about the intensity of turbulence, only about the yes/no presence of turbulence.

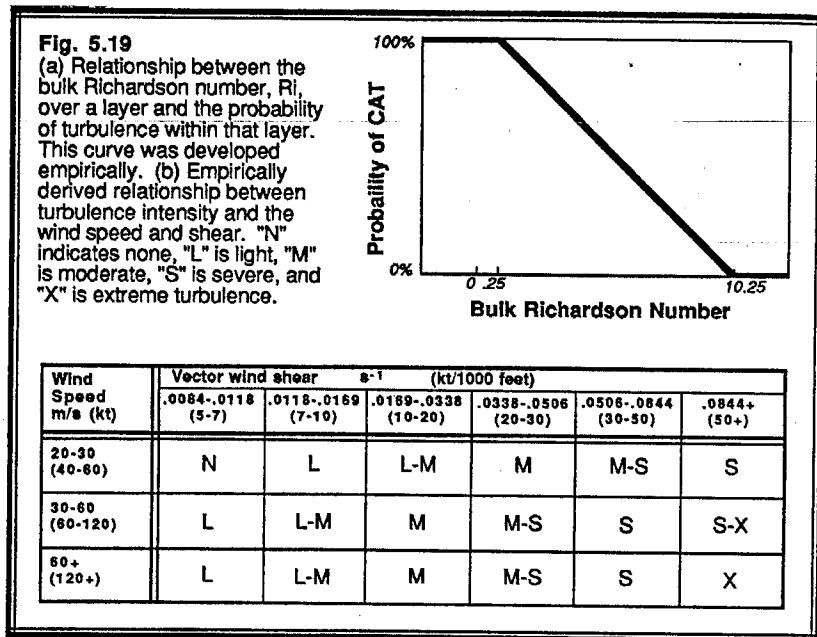


Fig 5.20 show examples of the evolution of the Richardson number during some nighttime case studies. Regions where the Richardson number is small are sometimes used as an indicator of the depth of the turbulent SBL. Here we see low Richardson numbers close to the ground, in addition to patches of low Richardson number aloft.

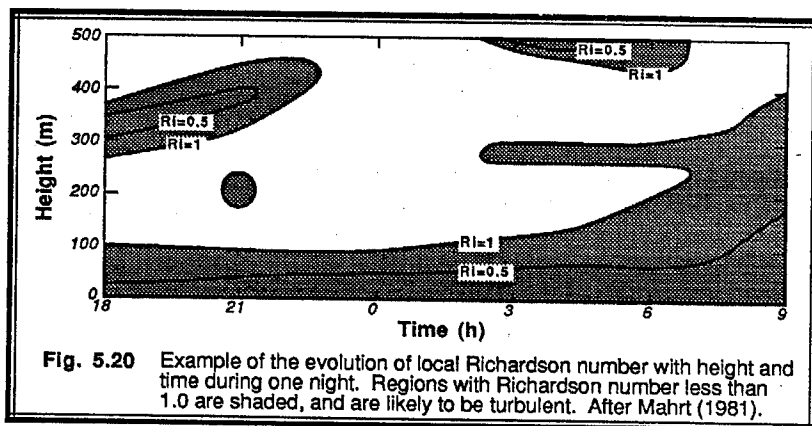


Table 5-1. Example of a nighttime rawinsonde sounding analyzed to give stability, shear, Richardson number, and the probability and intensity of turbulence. Probabilities are expressed as a percent, and intensities are abbreviated by:

N = no turbulence, L = light (0.5 G), M = moderate (1 G), S = severe (2 G)

These intensity levels correspond to the turbulence reporting recommendations used in aviation, where the vertical acceleration measured in Gs (number of times the pull of gravity) is relative to the center of gravity of the aircraft. For practical purposes, a probability greater than 50% AND an intensity greater than L were required before a CAT forecast would be issued.

z (m)	Wind Dir (°)	Wind Speed (m/s)	T (K)	θ (K)	Lapse (K/m)	Shear (s ⁻¹)	R _B	CAT Prob(%)	CAT Inten.
1591	154	9.8	281	294.4	0.0021	0.0034	6.19	41	N
1219	150	10.7	-	-	0.0021	0.0045	3.43	68	N
914	144	9.7	-	-	0.0021	0.0091	0.86	94	N-L
702	-	-	287.8	292.5	0.0020	0.0091	0.81	94	N-L
610	134	7.4	-	-	0.0020	0.0170	0.23	100	L-M
393	-	-	290.2	291.9	0.0204	0.0170	2.37	79	L-M
305	95	3.5	-	-	0.0204	0.0137	3.64	66	N
222	79	2.7	288.4	288.4	0.0133	0.0071	8.92	13	N
4	45	2.5	287.6	285.5	-	-	-	-	-

5.6.4 Examples

Problem A: Given the same data from problem 5.2.8, calculate the flux Richardson number and comment on the dynamic stability.

Solution. Since the flux Richardson number is defined as the ratio of the buoyancy term to the negative of the shear term, we can use the values for these terms already calculated in example 5.2.8:

$$R_f = \frac{\text{buoyancy term}}{-\text{shear term}} = \frac{0.00493}{-0.0003} = -16.4$$

Discussion. A negative Richardson number is without question less than +1, and thus indicates dynamic instability and turbulence. This is a trivial conclusion, because any flow that is statically unstable is also dynamically unstable by definition.

Problem B: Given a fictitious SBL where $(g/\bar{\theta}_v) = 0.033$, $\partial\bar{U}/\partial z = u_* / (kz)$, $u_* = 0.4$, and where the lapse rate, c_1 , is constant with height such that there is $6^\circ\text{C } \bar{\theta}_v$ increase with each 200 m of altitude gained. How deep is the turbulence?

Solution. We can use the gradient Richardson number as an indicator of dynamic stability and turbulence. Using the prescribed gradients, we find that:

$$Ri = \frac{\frac{g}{\bar{\theta}_v} \frac{\partial\bar{\theta}_v}{\partial z}}{\left(\frac{\partial\bar{U}}{\partial z}\right)^2} = \frac{\frac{g}{\bar{\theta}_v} c_1}{\left(\frac{u_*}{kz}\right)^2} = \frac{(0.033) \cdot (0.03)}{(0.4/0.4)^2} z^2 = (0.00099 \text{ m}^{-2}) z^2$$

If we use $R_c = 0.25$, then we can use this critical value in place of Ri above and solve for z at the critical height above which there is no turbulence:

$$z = \sqrt{(1010 \text{ m}^2) R_c} = \sqrt{252.5 \text{ m}^2} = 15.9 \text{ m}$$

Discussion. If we have used a critical termination value of $R_T = 1.0$, then we would have found a critical height of 31.8 m. Thus, below 15.9 m we expect turbulence, while above 31.8 m we expect laminar flow. Between these heights the turbulent state depends on the past history of the flow at that height. If previously turbulent, it is turbulent now.

5.7 The Obukhov Length

The Obukhov length (L) is a scaling parameter that is useful in the surface layer. To show how this parameter is related to the TKE equation, first recall that one definition of the surface layer is that region where turbulent fluxes vary by less than 10% of their magnitude with height. By making the constant flux (with height) approximation, one can use surface values of heat and momentum flux to define turbulence scales and nondimensionalize the TKE equation.

Start with the TKE equation (5.1a), multiply the whole equation by $(-k z/u_*^3)$, assume all turbulent fluxes equal their respective surface values, and focus on just terms III, IV, and VII:

$$\dots = \underbrace{-\frac{k z g (\overline{w'\theta_v'})_s}{\bar{\theta}_v u_*^3}}_{\text{III}} + \underbrace{\frac{k z (\overline{u_i' u_j'})_s}{u_*^3}}_{\text{IV}} + \dots - \underbrace{\frac{k z \epsilon|_s}{u_*^3}}_{\text{VII}} \quad (5.7a)$$

Each of these terms is now dimensionless. The last term, a dimensionless dissipation rate, will not be pursued further here.

The *von Karman constant*, k , is a dimensionless number included by tradition. Its importance in the log wind profile in the surface layer is discussed in the next section. Investigators have yet to pin down its precise value, although preliminary experiments suggest that it is between about 0.35 and 0.42. We will use a value of 0.4 in most of this book, although some of the figures adopted from the literature are based on $k=0.35$.

Term III is usually assigned the symbol, ζ , and is further defined as $\zeta \equiv z/L$, where L is the *Obukhov length*. Thus,

$$\zeta = \frac{z}{L} = \frac{-k z g (\overline{w'\theta_v'})_s}{\bar{\theta}_v u_*^3} \quad (5.7b)$$

The Obukhov length is given by:

$$L = \frac{-\bar{\theta}_v u_*^3}{k g (\overline{w'\theta_v'})_s} \quad (5.7c)$$

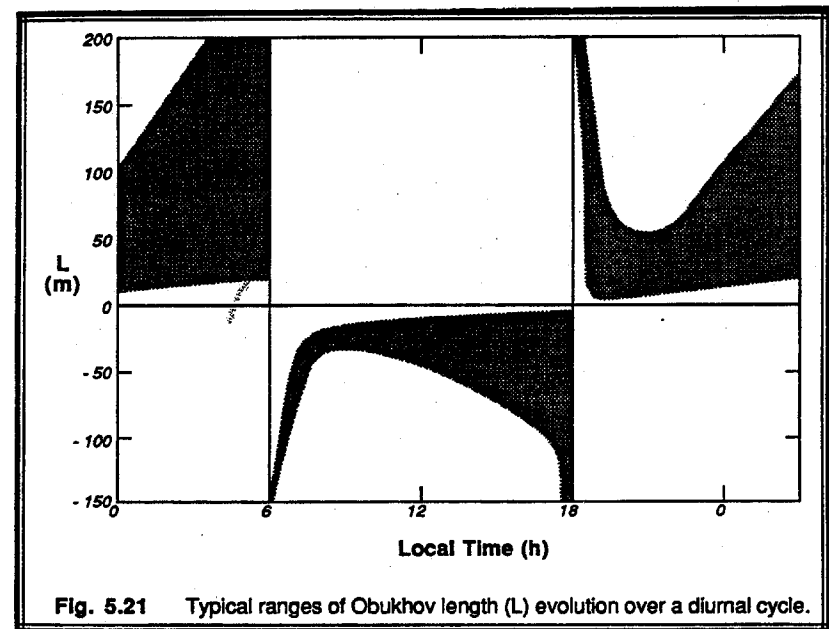


Fig. 5.21 Typical ranges of Obukhov length (L) evolution over a diurnal cycle.

$$\phi_H = \frac{kz}{\theta_*^{SL}} \frac{\partial \overline{\theta}_v}{\partial z} = \frac{(0.4)(10)}{(0.25)} (0.2) = 3.2$$

$$\mu = \frac{k u_*}{f_c L} = \frac{(0.4)(0.2)}{(10^{-4})(12)} = 66.7$$

5.10 Combined Stability Tables

Static and dynamic stability concepts are intertwined, as sketched in Fig 5.24a. Negative Richardson numbers always correspond to statically and dynamically unstable flow. This flow will definitely become turbulent. Positive Richardson numbers are always statically stable, but there is the small range of $0 < Ri < 1$ where positive Richardson numbers are dynamically unstable, and may be turbulent depending on the past history of the flow. Namely, nonturbulent flow will become turbulent at about $Ri = 0.25$, while flow that is presently turbulent will stay turbulent if $Ri < 1$.

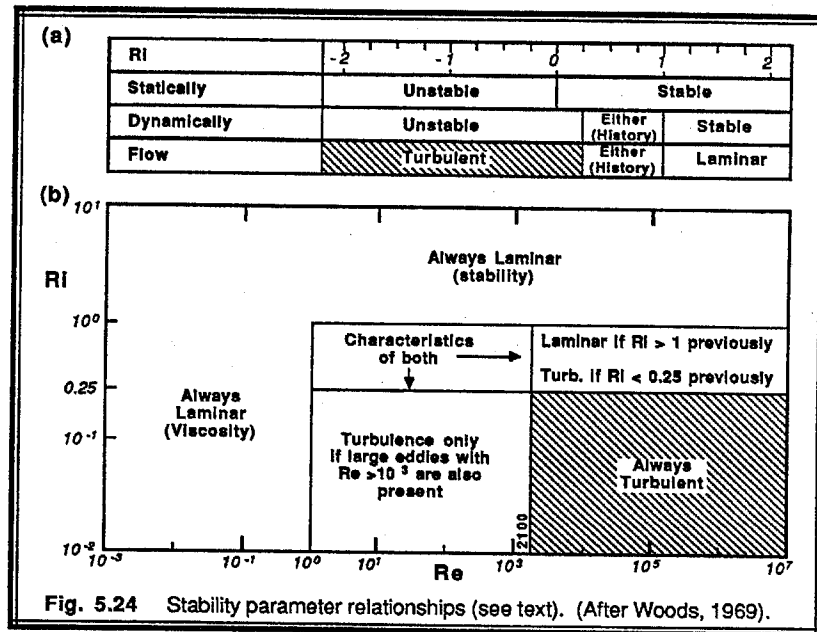


Fig. 5.24 Stability parameter relationships (see text). (After Woods, 1969).

The effects of viscosity and stability in suppressing turbulence are also intertwined, as sketched in Fig 5.24b. In Section 3.5.1 we defined the Reynolds number as the ratio of inertial to viscous forces, with no mention about buoyancy. In section 5.5.3, we defined a Richardson number as the ratio of buoyant to inertial or mechanical forces, with no mention of viscosity. In the atmosphere, the Reynolds number is usually so large that it corresponds to the rightmost edge of Fig 5.24b. Thus, we can essentially ignore viscous effects on stability in the atmosphere, and focus on the static and dynamic stability instead.

In conclusion, we see that the TKE equation is critical for determining the nature of flow in the BL. The relative contributions of various turbulence production and loss terms can be compared when rewritten as dimensionless scaling parameters. These parameters can be used to define layers within the BL where the physics is simplified, and where a variety of similarity scaling arguments can be made (see chapter 9 for details of similarity theory).

5.11 References

André, J.-C., G. De Moor, P. Lacarrère, G. Therry, and R. du Vachat, 1978: Modeling the 24-hour evolution of the mean and turbulent structures of the planetary boundary layer. *J. Atmos. Sci.*, **35**, 1861-1883.

Businger, J.A., J.C. Wyngaard, Y. Izumi and E.F. Bradley, 1971: Flux profile relationships in the atmospheric surface layer. *J. Atmos. Sci.*, **28**, 181-189.

Caughey, S.J., J.C. Wyngaard and J.C. Kaimal, 1979: Turbulence in the evolving stable boundary layer. *J. Atmos. Sci.*, **36**, 1041-1052.

Chou, S.-H., D. Atlas, and E.-N. Yeh, 1986: Turbulence in a convective marine atmospheric boundary layer. *J. Atmos. Sci.*, **43**, 547-564.

Deardorff, J.W., 1974: Three-dimensional numerical study of turbulence in an entraining mixed layer. *Bound.-Layer Meteor.*, **7**, 199-226.

Gal-Chen, T. and R.A. Kropfli, 1984: Buoyancy and pressure perturbations derived from dual-Doppler radar observations of the planetary boundary layer: applications for matching models with observations. *J. Atmos. Sci.*, **41**, 3007-3020.

Hechtel, L.M., 1988: The effects of nonhomogeneous surface heat and moisture fluxes on the convective boundary layer. *Preprints of the Am. Meteor. Soc. 8th Symposium on Turbulence and Diffusion in San Diego, April 1988*. 4pp.

Holtslag, A.A.M. and F.T.M. Nieuwstadt, 1986: Scaling the atmospheric boundary layer. *Bound.-Layer Meteor.*, **36**, 201-209.

Kitchen, M., J.R. Leighton and S.J. Caughey, 1983: Three case studies of shallow convection using a tethered balloon. *Bound.-Layer Meteor.*, **27**, 281-308.

Lee, D.R., R. B. Stull, and W.S. Irvine, 1979: *Clear Air Turbulence Forecasting Techniques*. AFGWC/TN-79/001. Air Force Global Weather Central, Offutt AFB, NE 68113. 73pp.

Lenschow, D.H., 1974: Model of the height variation of the turbulence kinetic energy budget in the unstable planetary boundary layer. *J. Atmos. Sci.*, **31**, 465-474.

Lenschow, D.H., J.C. Wyngaard and W.T. Pennell, 1980: Mean field and second